

Comparative study of Pb (II) adsorption from water on used cardboard and powdered activated carbon

Fouad. Mekhalef Benhafsa^{1,2,3}, Abdelghani. Bouchama^{*1,3}, Aicha. Chadli⁴, Belgacem. Tadjer¹ and Djelloul. Addad⁵

¹Centre de Recherche Scientifique et Technique en Analyses Physico-chimiques CRAPC, BP 384, Bou-Ismaïl, 42004, Tipaza, Algeria

²Laboratory of Advanced Materials and Physicochemistry for the Environment and Health (MAPES),
Djillali Liabes University, P.B. 89 Sidi Bel Abbes 22000, Algeria

³Laboratoire de Structure, Elaboration et Application des Matériaux Moléculaires (SEA2M), Faculté des Sciences et de la Technologie,
BP 188, Université Abdelhamid Benbadis, Mostaganem, Algeria

⁴Biotechnology applied laboratory to agriculture and environmental preservation, higher school of agronomy,
Ex-hall of technology kharoubba, Mostaganem (27000), Algeria

⁵Laboratoire des Eco Matériaux Fonctionnels et Nanostructurés, Université de Mohammed Boudiaf, Oran, Algeria

(Received October 24, 2021, Revised January 17, 2022, Accepted January 19, 2022)

Abstract. In the present study, we compared the adsorption capacity of Pb (II) from contaminated water of used cardboard (UC) and a commercial powdered activated carbon (PAC), the latter has been characterized by different techniques, namely X-ray diffraction (XRD), scanning electron microscopy with energy dispersive spectroscopy (SEM/EDS), wavelength dispersion x-ray fluorescence (WDXRF), infrared spectroscopy (IR) and surface area B.E.T analyzer. The effect of various parameters, such as the pH, the contact time, the amount of adsorbent, and the temperature on the adsorption of Pb (II) on both materials was investigated. The Pb (II) adsorptions are perfectly described by a pseudo-second-order model, while the intraparticle diffusion is a decisive step after the first minutes of contact. The fit to the Langmuir and Redlich-Peterson models seems perfect for these adsorption reactions. (PAC) showed a greater affinity for Pb (II) compared to (UC) and the adsorption of Pb (II) ions is strongly pH-dependent, on the other hand, the increase in temperature doesn't have much influence on the two solids. This study showed that the capacity of (UC) to adsorb Pb (II) from an aqueous solution is greater than two-thirds of that of (PAC).

Keywords: adsorption; modeling; Pb (II); powdered activated carbon; used cardboard

1. Introduction

Many industries such as electroplating, battery manufacturing, mining, explosives manufacturing, electronics, metallurgy, pesticides, and petroleum refining, use heavy metals in the manufacture of their products. Consequently, these toxic and non-biodegradable metals will pollute the aquatic environment, the presence of these pollutants in the water, even in trace amounts, is highly undesirable (Rashed *et al.* 2018, Herawati *et al.* 2000), because they accumulate in the living tissues of the human body, causing diverse sickness and crucial physiological disorders such as damage to the central nervous system (Mohammadi *et al.* 2010, Axtell *et al.* 2003). Pb is one of the most common and toxic heavy metal pollutants (Hana *et al.* 2020) Ingestion, inhalation, or skin absorption of Pb ions causes acute poisoning and many serious problems such as edema, anemia, childhood learning disabilities, and kidney disease (Sreejalekshmi *et al.* 2009), therefore, the contamination of natural, industrial or wastewater by heavy metals is a topic that has attracted the attention of many environmental scientists around the world using a wide

variety of techniques including biological processes, membrane separation processes, chemical precipitation, ion exchange, electrodeposition, oxidation-reduction, complexation, reverse osmosis, etc. (Amarasinghe and Williams 2007)

All of these methods are generally expensive, moreover, some processes such as precipitation and membrane filtration encounter enormous difficulties in removing heavy metals from water, as they are not effective at high concentrations of pollutants, hence, these methods have become less attractive and the development of new economical and environmentally friendly methods has become a priority (Ayyappan *et al.* 2005). From an economic and environmental point of view, adsorption has proven to be an excellent method for removing heavy metals from wastewater, due to its significant advantages such as low cost, efficiency, and ease of use, compared to traditional methods. (Crini and Badot 2010, Özcan *et al.* 2006, Ponnusamy and Subramaniam 2013)

Several mineral materials such as clays (Bouberka *et al.* 2005, Georgescu *et al.* 2018), zeolites (Elboughdiri 2020), or organic such as synthetic polymers (Jeongmin *et al.* 2020) and biopolymers (Chionyedua *et al.* 2019), or composites such as zinc nanoparticles (Kataria *et al.* 2016) have been tested on a laboratory scale.

Activated carbons characterized by their high surface area and their microporous nature and due to their excellent

*Corresponding author, Ph.D.,
E-mail: bouchama.abdelghani@crapc.dz

adsorption power are the most widely used as adsorbents.

These very broad-spectrum materials are capable of interacting effectively with almost all pollutants, especially heavy metals. However, the processes using commercial activated carbon have drawbacks, namely their price, their rapid saturation, the problems of disposal after use, and their regeneration which is very expensive in energy, leading to real economic problems (Hashemian 2011, Shirsath and Shrivastava 2012). In recent years and a global context of a reduction in the volume of waste, the reuse of manufacturing co-products or of waste itself has been a priority in terms of sustainable development. Waste is an unused resource and, in many cases, poses serious disposal problems (Bharathi and Ramesh 2012). In this context, many studies have been conducted to preserve the environment, as well as to replace expensive adsorbents with other low-cost, environmentally friendly materials, called unconventional adsorbents such as peat, biomass, agricultural residues, chitin, chitosan, coconut, wheat bran, date stones, sawdust, and pistachio shells. (Sepulveda and Santana 2013, Mekhalef Benhafsa *et al.* 2018, Bai *et al.* 2020, Obayomi *et al.* 2019, Boulaiche *et al.* 2019, Brião *et al.* 2020)

This work aims at the possibility of using household waste from corrugated cardboard to eliminate a metallic element, Pb, in an aqueous solution, and to evaluate its adsorbance compared to the universal adsorbent, powdered activated carbon. Different experimental conditions influencing the retention phenomenon, such as contact time, sorbent dosage, pH, and temperature, were adjusted. Kinetic adsorption models, equilibrium isotherms models, and thermodynamic parameters were also evaluated.

2. Materials and methods

2.1 Materials

The used cardboard (UC) used in this study was obtained from the market, in the form of packaging waste of certain products, it is corrugated cardboard, its walls are made of sheets of corrugated paper glued to one or between several cardboard sheets. After being cut into small pieces and removing the printed parts, the (UC) was air-dried, then pulverized and sieved to extract particles with a diameter of fewer than 200 μm . The selected fraction was dried at 80°C for 48 h, then cooled in a desiccator, and finally stored in sealed plastic bags.

The fine powdered activated carbon (PAC) with a diameter of fewer than 45 μm was purchased from Sigma Aldrich, the material was washed with continuous stirring for one hour with distilled water, then allowed to stand, and the precipitate was collected after one hour. The process was repeated 5 times. Finally, the sample was dried at 80°C for 24 hours, then cooled and stored in a desiccator to prevent moisture absorption.

Lead nitrate $\text{Pb}(\text{NO}_3)_2$ (99,5%), sodium hydroxide pellets NaOH (97%) a nitric acid HNO_3 ($\geq 65\%$) were purchased from AnalaR Analytical reagent, Panreac, and Honeywell chemicals respectively.

2.2 Characterization

The microstructural analysis of the materials was carried out using a Quanta 250 type scanning electron microscope, coupled with a complete EDS microanalysis analytical system of the EDAX AMTEK brand and the Octane Pro type. The sample is bombarded by an electron beam with an energy of around 20 keV. The spatial resolution of the analysis and the depth analyzed are in the order of 10 μm .

Fourier transform infrared spectra (FTIR) were recorded from 400 to 4000 cm^{-1} using a BRUKER α ALPHA-T FT-IR spectrophotometer.

XRD powder patterns were collected on a BRUKER D8 ADVANCE diffractometer using the monochromatic $\text{Cu K}\alpha$ radiation of copper ($\text{Cu K}\alpha$ -radiation) ($\lambda = 1.5406 \text{ \AA}$, voltage 40 KV, and current 40 mA), the diffraction angle (2θ) varied from 5° to 100° with a step width of 0.04°.

The elemental composition of (UC) was analyzed by wavelength dispersion x-ray fluorescence spectrometer (ZSX Primus II by Rigaku) with Rhodium anticathode. Before the analysis, the powdered (UC) was transformed into a pellet of 30 mm in diameter by applying a force of 10 KN by a SPECAC compressor.

The specific surface of the used cardboard was carried out by a Micromeritics ASAP 2020 device, based on the application of the BET model to a type II isotherm, the samples were degassed for 6 hours at 80°C.

The pH measurement was effectuated using an ISKRA MA laboratory digital pH meter, calibrated with buffer solutions of pH 4 and pH 7.

The point of zero charges (pH_{pzc}) can be defined as the pH of the suspension at which a surface has a net zero charge (Sparks 2003). To determine the pH_{pzc} value of (UC) aliquots with 50ml of 0.01 M NaCl solution were prepared in different vials and the initial pH was adjusted from 2 to 12 by adding 1N solution of NaOH or HCl, 0.15 g of adsorbent sample was added to each flask and the suspensions were then stirred for 48 hours at room temperature. The curve of the final pH versus the initial pH was plotted, the pH_{pzc} value is the intersection point of this curve with the line $\text{pH}_{\text{final}} = \text{pH}_{\text{initial}}$ (Singh 2011).

The determination of the Pb (II) ions concentration was carried out by atomic absorption spectrophotometry using an Agilent AA 240FS model flame atomic absorption spectrophotometer.

2.3 Adsorption experiments

The adsorption experiments of Pb (II) onto the two solids and the influence of various parameters were realized using the batch technique. For each experiment, a given quantity of the adsorbent was brought into contact with 100 ml of solutions at an initial concentration C_0 of Pb (II) ions. Using a magnetic stirrer, the mixture was stirred for well-established intervals of time at a speed of 600 rpm at a temperature of $25 \pm 2^\circ\text{C}$. Finally, the adsorbent was separated from the contaminated solution by filtration, and Pb (II) ions concentration from the filtrate was determined by atomic absorption spectrophotometer.

The adsorption percentage and the adsorbed amount of

metal ions were calculated by Eqs. (1) and (2) respectively.

$$\% \text{ adsorption} = \frac{(C_0 - C_e)}{C_0} \times 100 \quad (1)$$

$$Q_e = \frac{(C_0 - C_e)V}{W} \quad (2)$$

where C_0 is the initial concentration of the Pb (II) ions solution in ($\text{mg}\cdot\text{L}^{-1}$). C_e is the equilibrium concentration of the Pb (II) solution in ($\text{mg}\cdot\text{L}^{-1}$). V is the volume of the solution in (L), W is the mass of adsorbent in (g), and Q_e is the amount adsorbed in ($\text{mg}\cdot\text{g}^{-1}$).

2.3.1 Effect of adsorbent amount

The effect of the amount of each material was studied for the adsorption of Pb (II) ions from a $20 \text{ mg}\cdot\text{L}^{-1}$ solution at different doses of adsorbent ranging from 0.01 to 0.19 g/100ml. The mixture was stirred for one hour at a temperature of $25 \pm 2^\circ\text{C}$ and an initial pH of 5.3. After the separation of the solids from the solution, the filtrates were analyzed to determine the quantities of residual Pb (II).

2.3.2 Effect of the initial pH of the solution

The influence of pH on the adsorption of Pb (II) ions on used cardboard and powdered activated carbon separately, was studied at an initial concentration of Pb (II) ions of $20 \text{ mg}\cdot\text{L}^{-1}$ and 0.14 g of used cardboard and 0.08 g for the powdered activated carbon. The initial pH of the polluted solutions was adjusted with HNO_3 (1N) and NaOH (1N) to reach values from 2 to 12.

2.3.3 Effect of contact time and kinetics

The effect of contact time on the adsorption process was investigated at varied times between 0 and 240 min at initial pH (5.6) using 100 mL Pb (II) ions solutions with initial concentrations of $20 \text{ mg}\cdot\text{L}^{-1}$ and 0.14 g of (UC) and 0.08 g for the second adsorbent (PAC) at a temperature of $25 \pm 2^\circ\text{C}$ with stirring at a speed of 600 rpm. The variation of the concentrations of the Pb (II) solutions was checked at the given time intervals. The mixtures were then filtered to remove adsorbent particles and their Pb (II) concentrations were determined by atomic absorption spectrophotometry (AAS) at $\lambda = 217 \text{ nm}$.

Three kinetic models were applied for the experimental data in this study, namely pseudo-first-order, pseudo-second-order, and intraparticle diffusion.

The pseudo-first-order kinetic model of Lagergren (1898) is expressed by the Eq. (3):

$$\log(Q_e - Q_t) = \log Q_e - \frac{k_1}{2,303} t \quad (3)$$

where, Q_t and Q_e in ($\text{mg}\cdot\text{g}^{-1}$) are the amounts of adsorbate extracted at times t and at equilibrium, respectively, k_1 (min^{-1}) is the pseudo-first-order rate constant.

The linearized pseudo-second-order Eq. (4) is calculated according to Ho and Mckay (1999), as follows:

$$\frac{t}{Q_t} = \frac{1}{k_2 Q_e^2} + \frac{1}{Q_e} t \quad (4)$$

where, Q_t and Q_e expressed in ($\text{mg}\cdot\text{g}^{-1}$) are the amounts of Pb (II) ions extracted at times t and at equilibrium, respectively, k_2 ($\text{mg}\cdot\text{g}^{-1}\cdot\text{min}^{-1}$) is the pseudo-second-order rate constant. This equation is based on the sorption capacity of the solid phase and this model assumes that chemisorption can be the flow control step in adsorption processes (Simonin 2016).

The intraparticle diffusion model was also tested to verify what is the limiting step of the adsorption process (Weber and Morris 1963), the intraparticle diffusion rate constant (K_{id}) is determined using Eq. (5).

$$Q_t = k_{id} t^{1/2} + C \quad (5)$$

where K_{id} ($\text{mg}\cdot\text{g}^{-1}\cdot\text{min}^{-1/2}$) is the intraparticle diffusion rate constant and C ($\text{mg}\cdot\text{g}^{-1}$) is a constant which may indicate the thickness of the boundary layer, the higher the constant C , the greater the boundary layer effect (El-Ashtoukhy *et al.* 2008, Kanan and Sundaram 2001). Moreover, if the graphical representation of Q_t as a function of $t^{1/2}$ gives a straight line, the sorption process will be controlled by intraparticle diffusion only. However, if the data shows multi-line graphs, two or more steps influence the sorption process (Srivastava *et al.* 2006).

2.3.4 Effect of temperature

The influence of temperature on the elimination of Pb (II) ions from water polluted by the two adsorbents was studied between 25 and 55°C using volumes of 100 ml of lead nitrate solution concentrated at $20 \text{ mg}\cdot\text{L}^{-1}$ of Pb(II) at the initial pH of solutions and 0.14 g of used cardboard for each experiment and 0.08 g of adsorbent in the case of powdered activated carbon. After stirring to equilibrium and filtering the supernatants, an absorbance reading corresponding to each solution was taken by an atomic absorption spectrophotometer calibrated to the Pb excitation wavelength of 217 nm.

2.3.5 Adsorption isotherm models

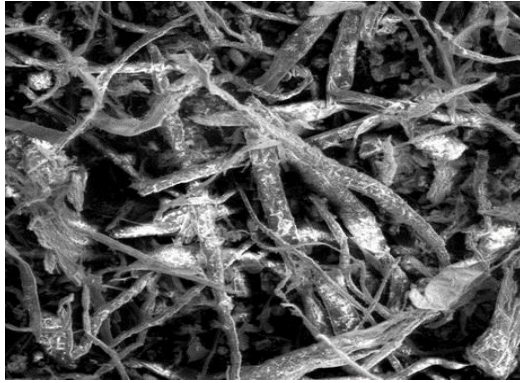
The purpose of this study is to determine the maximum adsorption capacity of 1 g of solid and subsequently to identify the type of adsorption, it was carried out by adding 0.14 g of (UC) and 0.08 g of (PAC) in vials containing 100 mL of Pb(II) solutions with initial concentrations between $9 \text{ mg}\cdot\text{L}^{-1}$ and $65 \text{ mg}\cdot\text{L}^{-1}$ for (UC) and between 10 and $90 \text{ mg}\cdot\text{L}^{-1}$ for (PAC), these flasks were kept stirred at 600 rpm at a temperature of $25 \pm 2^\circ\text{C}$ and initial pH = 5.

A contact time of 10 minutes for (UC) and 20 minutes for (PAC) was respected.

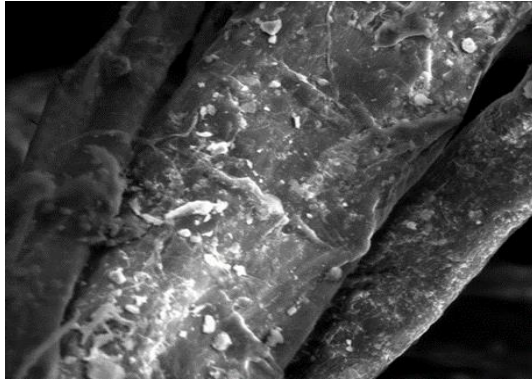
After treatment, the residual concentration of Pb (II) ions in the solution at equilibrium (C_e) was measured by atomic absorption spectrophotometry and the adsorption capacity (Q_e) was determined using Eq. (2).

To model the adsorption isotherm, we have adopted four well-known models: that of Langmuir (1918), Freundlich (1907), Elovich and Larionov (1962), and Redlich and Peterson (1959) whose linear equations can be written respectively as follows:

$$\frac{C_e}{Q_e} = \frac{1}{Q_m} C_e + \frac{1}{K_L Q_m} \quad (6)$$



(a) 400-times magnification Wind speed profile



(b) 5000-times magnification

Fig. 1 SEM image of used cardboard

$$\ln Q_e = \ln K_F + \left(\frac{1}{n}\right) \cdot \ln C_e \quad (7)$$

$$\ln\left(\frac{Q_e}{C_e}\right) = \ln(K_E)Q_m - \frac{Q_e}{Q_m} \quad (8)$$

$$\frac{C_e}{Q_e} = \frac{1}{Q_m K_L} + \frac{K_L^{n-1}}{Q_m} C_e^n \quad (9)$$

3. Results and discussion

3.1 Used cardboard characterization

Morphological analysis of (UC) by a scanning electron microscope (SEM) showed that this material has a filamentary structure resulting from the presence of cellulosic fibers made up of a series of D-glucose molecules. These filaments are both short and long and relatively wide and thick. They are arranged randomly revealing cavities and channels Fig. 1.

The FT-IR spectrum of used cardboard recorded between 400 and 4000 cm^{-1} (Fig. 3) shows the characteristics of cellulose (Hospodarova *et al.* 2018), including the broadbands between 3320-3330 cm^{-1} resulting from the elongation vibration of the O-H bond. Those observed at 872 and 659 cm^{-1} are characteristic of the shear deformation of the C-H bond in the aromatic ring. The absorption band

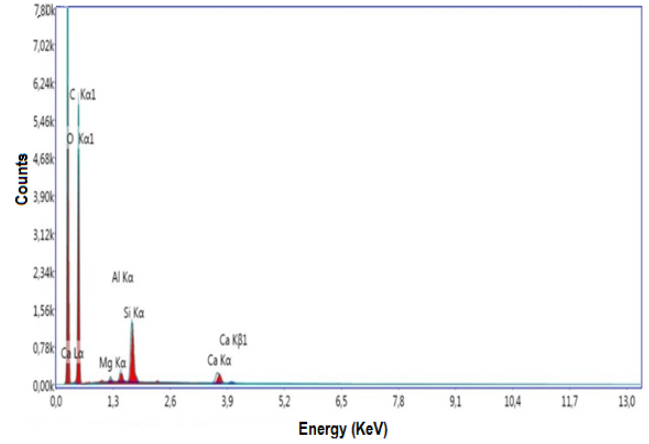


Fig. 2 EDX spectrum of used cardboard

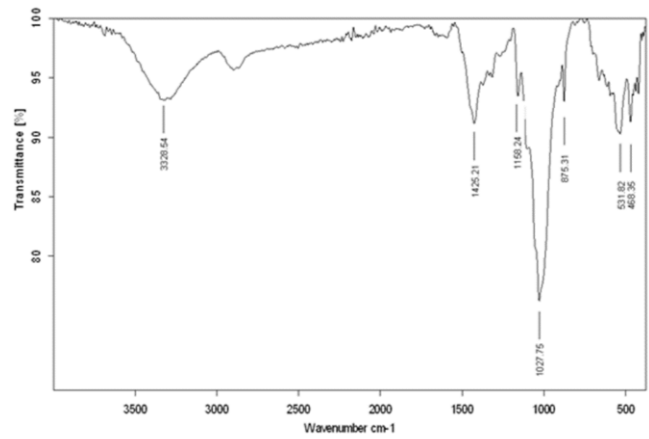


Fig. 3 FTIR spectrum of used cardboard

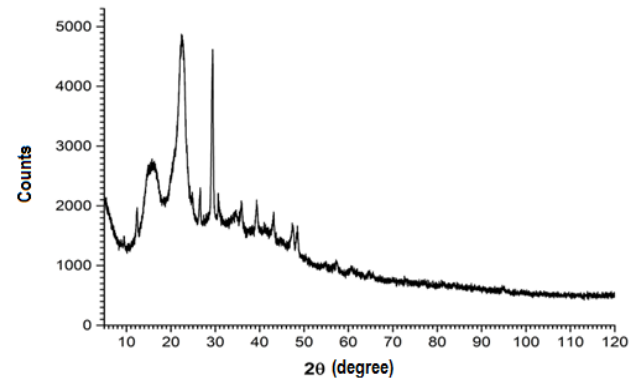


Fig. 4 XRD spectrum of used cardboard

due to the deformation vibration of water molecules can be attributed to that observed around 1580 cm^{-1} . The vibrations of the C-C bond of the aromatic ring are distinguished by the absorption band at 1425 cm^{-1} . The characteristic bands associated with the O-C-C stretching vibration appear at 1158 and 1160 cm^{-1} .

Fig. 4 illustrates the XRD spectrum of the (UC). The result obtained from this analysis shows that 57.1% of our material is in an amorphous state and 42.9% is in a crystalline state. The low crystallinity of (UC) does not allow it to develop a large specific surface. The XRD

Table 1 WDXRF analysis of (UC) elementary composition

Elements	Weight (%)	Elements	Weight (%)
C	37.2696	Cr	0.0058
O	53.8808	Mn	0.0053
Na	0.1368	Fe	0.2489
Mg	0.3637	Ni	0.0012
Al	1.1915	Cu	0.0041
Si	1.9391	Zn	0.0087
P	0.0156	Br	0.0008
S	0.1725	Sr	0.0043
Cl	0.0608	Y	0.0004
K	0.0893	Zr	0.0019
Ca	4.5274	Pb	0.0021
Ti	0.0694		

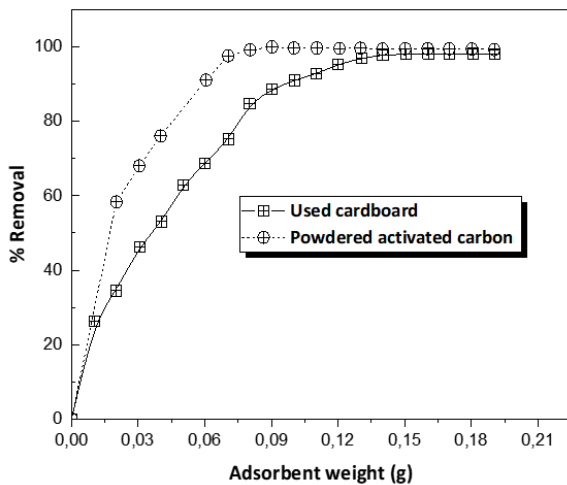


Fig. 5 Effect of the adsorbent dosage on Pb (II) removal from aqueous solution ($C_0 = 20 \text{ mg}\cdot\text{L}^{-1}$, $m_{(\text{UC})} = 0.14 \text{ g}$, $m_{(\text{PAC})} = 0.08 \text{ g}$, $V = 100 \text{ mL}$, $t = 1 \text{ h}$, $v = 600 \text{ rpm}$, $\text{pH}_{\text{initial}} = 5.3$, $T = 25 \pm 2^\circ\text{C}$)

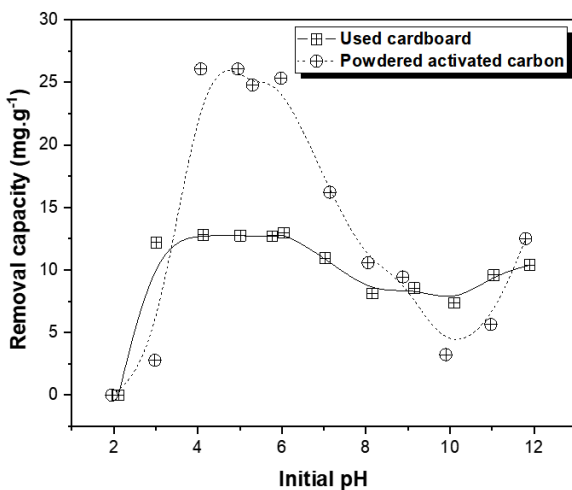


Fig. 6 Effect of initial pH of the solutions on Pb (II) ions extracted amounts ($C_0 = 20 \text{ mg}\cdot\text{L}^{-1}$, $m_{(\text{UC})} = 0.14 \text{ g}$, $m_{(\text{PAC})} = 0.08 \text{ g}$, $V = 100 \text{ mL}$, $t = 1 \text{ h}$, $v = 600 \text{ rpm}$, $T = 25 \pm 2^\circ\text{C}$)

diffractogram of the sample shows several characteristic peaks of cellulose, calcite, and ammoniacal cellulose, the content of which is respectively equal to 50.0, 36.5 and 13.4%.

The specific surface of (UC), determined at the relative pressure $p/p_0 = 0.296026227$, is equal to $1.0192 \text{ m}^2\cdot\text{g}^{-1}$. The total volume of pores with a diameter of less than 187.21 nm, determined at $p/p_0 = 0.989661564$, is $0.003640 \text{ cm}^3\cdot\text{g}^{-1}$ and the average pore width is 14.28481 nm. The average particle size is around $5.886 \mu\text{m}$.

Table 1 shows the WDXRF analysis results, the weight fractions of the various elements present in the (UC), it can be seen in this table that the majority of the elements are oxygen and carbon.

The determined pH_{pzc} value is 7.93, so at $\text{pH} < 7.93$, the surface of the (UC) has a net positive charge, while at $\text{pH} > 7.93$ the surface has a net negative charge.

3.2 Effect of adsorbent dosage

The effects of the concentration of (UC) and (PAC) on the percentage of Pb (II) ions adsorbed from the solution are shown in Fig. 5. The results show that by increasing the dosage of (UC) from 0.01 to 0.14 g and (PAC) from 0.01 to 0.08 g, the percentage of elimination of Pb (II) ions increased from 26.26% to 97.86% and from 13.37% to 99.22% respectively, this could be attributed to the increase in the adsorbent surface and the availability of more adsorption sites (Alshameri *et al.* 2014, Shaban *et al.* 2018, Battas *et al.* 2019, Xia *et al.* 2018). It was observed that there was no significant increase in the percentage of elimination beyond 0.14 g of (UC) and 0.08 g of (PAC). Therefore, 0.14 g of (UC) and 0.08 g of (PAC) in 100 ml of Pb (II) solution were used for subsequent adsorption studies.

3.3 Effect of initial pH

The solution pH is an important variable governing the adsorption process, it influences not only the degree of ionization of the adsorbate but also the surface charge of the adsorbent particles present in the solution. The effect of pH on the adsorption of Pb (II) ions onto the (UC) and the (PAC) is presented in Fig. 6, which shows the variations in the Pb (II) quantities extracted (Q_e) as a function of the initial pH of solutions. In the initial pH range between 2 and 4, there is a strong improvement in the adsorption process as the pH increases, with better adsorption efficiency at pH between 4 and 6. The retention rate of Pb (II) ions increases with the increase in pH to reach a maximum elimination of 97% towards a pH of 5 with an extracted quantity of Pb (II) of the order of $12.75 \text{ mg}\cdot\text{g}^{-1}$ for the (UC) and 99.3% with an extracted quantity of $26 \text{ mg}\cdot\text{g}^{-1}$ for (PAC). At low pH, the adsorbents used are positively charged since the pH is below isoelectric points. Therefore, the electrostatic repulsive forces between H_3O^+ and Pb (II) reduce the removal yields of Pb (II) ions (Hameed 2009). At higher pH values, the adsorbent's surfaces become negatively charged due to deprotonation, causing strong electrostatic attraction which promotes high absorption of Pb (II) (Nejadshafiee

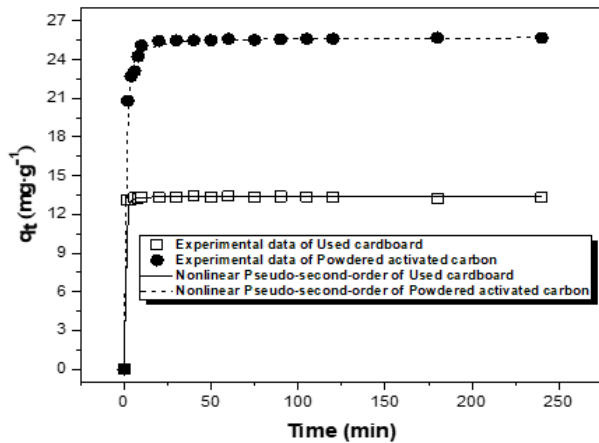


Fig. 7 Effect of contact time and the nonlinear fitting curves of Pseudo-second-order kinetics ($C_0 = 20 \text{ mg}\cdot\text{L}^{-1}$, $m_{(\text{UC})} = 0.14 \text{ g}$, $m_{(\text{PAC})} = 0.08\text{g}$, $V = 100 \text{ mL}$, $v = 600 \text{ rpm}$, $\text{pH}_{\text{Initial}} = 5.6$, $T = 25\pm 2^\circ\text{C}$)

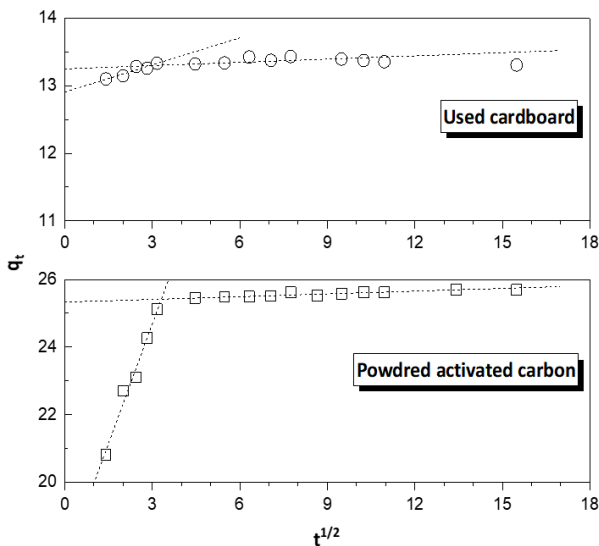


Fig. 8 Adjustment of Pb(II) ions adsorption onto (UC) and (PAC) to the intra-particle diffusion model

Table 2 Kinetic parameters of Pb(II) ions adsorption on (UC) and (PAC)

Kinetic models	Kinetic parameters	Kinetic parameters values	
		Used cardboard	Powdered activated carbon
Pseudo-first-order	$K_1 \text{ (min}^{-1}\text{)}$	0.00260	0.02501
	$Q_e \text{ (cal) (mg}\cdot\text{g}^{-1}\text{)}$	0.10	1.14
	r^2	0.02671	0.79572
Pseudo-second-order	$K_2 \text{ (g}\cdot\text{mg}^{-1}\cdot\text{min}^{-1}\text{)}$	0.78330	0.08764
	$Q_e \text{ (cal) (mg}\cdot\text{g}^{-1}\text{)}$	13.43	25.74
	r^2	0.99999	1
Intra-particle diffusion	$K_{id} \text{ (mg}\cdot\text{g}^{-1}\cdot\text{min}^{-1/2}\text{)}$	0.01596	0.02711
	$C \text{ (mg}\cdot\text{g}^{-1}\text{)}$	13.25	25.33
	r^2	0.96722	0.9854
Experimental data	$Q_{e(\text{exp})} \text{ (mg}\cdot\text{g}^{-1}\text{)}$	13.43	25.69

and Islami 2019). The curve records a decrease in the quantities extracted at pH greater than 6, this can be explained by the precipitation of Pb(II) ions in the form of lead hydroxide $\text{Pb}(\text{OH})_2$, basic nitrates: $\text{Pb}(\text{NO}_3)_2\cdot\text{Pb}(\text{OH})_2$ and $\text{Pb}(\text{NO}_3)_2\cdot 5\text{Pb}(\text{OH})_2$. Therefore, pH 5 was chosen as the optimum pH.

3.4 Effect of contact time and Adsorption kinetics study

The effect of contact time on the adsorption capacity of Pb(II) ions was studied to establish equilibrium time and adsorption kinetics. The adsorption of Pb(II) ions against time onto the (UC) and (PAC) is shown in Fig. 7.

The adsorption on the (UC) is very high in the first minutes; 97% of Pb(II) ions were adsorbed after only 2 min. This is mainly attributed to the electrostatic attraction between the Pb(II) ions and the surface of (UC), and the sufficient availability of free active sites at the initial period, which causes efficient adsorption. On the other hand, the fixing of Pb(II) ions on (PAC) seem to be slower compared to (UC) in the first minutes of contact where the percentage retained was 97% after 10 minutes of stirring. Over time, the retention becomes slow and regular, and because of the greater chemical interactions and interionic forces which slow the movement of the ions, the remaining vacant sites become difficult to be occupied by the Pb(II) ions. We retain at these times that one gram of (UC) can fix 13.33 mg of Pb(II), approximately half of the quantity fixed by the (PAC) which is 25.46 mg which represents about 99% elimination for both solids. The experimental data can confirm that the Pb(II) transfer takes place in two stages, the external or superficial diffusion which is expressed more particularly during the first minutes of contact between the liquid and solid phase. During this step, the Pb(II) ions attach themselves to the outer surface of the (UC) and (PAC) particles, and then a slow step corresponds to the diffusion of the Pb(II) ions inside the pores of the solid particles. Maier and Schure (2018) showed that the effective diffusion coefficient is high near the shell of the particle, which is widely open to the interstitial flow and decreases with depth in the particle.

To study the mechanism controlling adsorption processes, the kinetic data collected in this study were adapted to three two-parameter kinetic models.

According to the calculated values of k_1 , Q_e , and the correlation coefficient (r^2) given in Table 2, it turns out that the pseudo-first-order model does not reflect well the reaction of Pb(II) ions adsorption by (UC) and (PAC), the Q_e values calculated by applying this model are equal to $0.10 \text{ mg}\cdot\text{g}^{-1}$ for (UC) and $1.14 \text{ mg}\cdot\text{g}^{-1}$ for (PAC), they are very far compared to the quantities set at equilibrium recorded experimentally which are of the order of $13.43 \text{ mg}\cdot\text{g}^{-1}$ and $25.69 \text{ mg}\cdot\text{g}^{-1}$, respectively.

The kinetic parameters fitted to the pseudo-second-order graph shown in Fig. 7 for the removal of Pb(II) ions by (UC) and by (PAC) at $25 \pm 2^\circ\text{C}$ are presented in Table 2.

The pseudo-second-order kinetic model best matches the kinetic data for the two adsorbents with a correlation coefficient (r^2) very close or equal to unity. The calculated Q_e values are of the order of $13.43 \text{ mg}\cdot\text{g}^{-1}$ for (UC) and

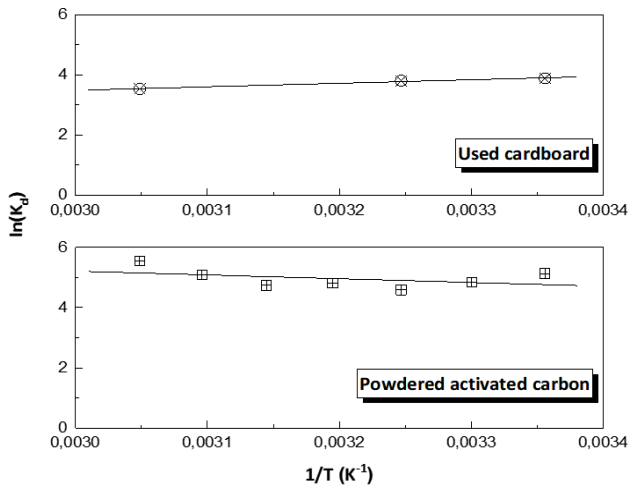


Fig. 9 Temperature effect on the adsorption of Pb (II) ions onto (UC) and (PAC) ($C_0 = 20 \text{ mg}\cdot\text{L}^{-1}$, $m_{\text{UC}} = 0.14 \text{ g}$, $m_{\text{PAC}} = 0.08 \text{ g}$, $V = 100 \text{ mL}$, $t_{\text{UC}} = 10 \text{ min}$, $t_{\text{PAC}} = 20 \text{ min}$, $v = 600 \text{ rpm}$, $\text{pH}_{\text{initial}} = 5.6$).

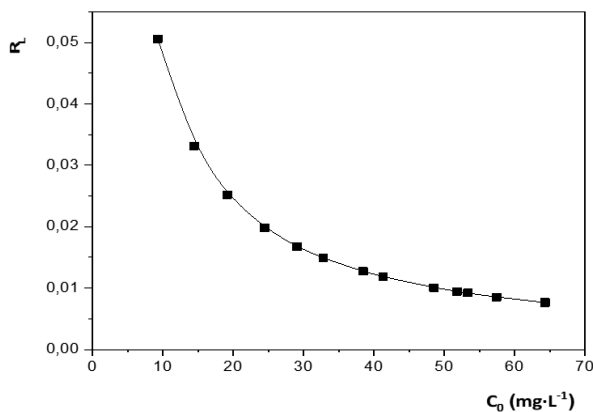


Fig. 10 Variation of R_L as a function of C_0 for used cardboard

$25.74 \text{ mg}\cdot\text{g}^{-1}$ for (PAC), they are very close to those obtained experimentally which are respectively $13.43 \text{ mg}\cdot\text{g}^{-1}$ and $25.69 \text{ mg}\cdot\text{g}^{-1}$. This order of reaction suggests chemisorption, the intraparticle diffusion of which may play an important role in the control of this process.

The plot of Q_t versus $t^{1/2}$ is shown in Fig. 8. The K_{id} values, as well as the correlation coefficients r^2 , are given in Table 2. It is easy to see from Fig. 8 that the experimental points are organized in two lines, the first, during the first minutes, can be attributed to the effects of diffusion in the boundary layer or the effects of external mass transfer (Mckay *et al.* 1980). The second line, which appears after the first 7 minutes of stirring for (UC) and after the first 11 minutes for (PAC) and persists throughout the process, represents diffusion into micropores (Allen *et al.* 1989). This latency can be explained by the movement of Pb (II) ions in the micropores of the carbon and the channels of the cellulosic fibers of the used cardboard, before arriving at the surface where they will be arranged in layers along the fibers. The deviation of the lines from the origin may be due to the difference in the rate of mass transfer at the initial and final stages of adsorption. Also, such a deviation of the

straight line from the origin indicates that pore diffusion is not the only step in controlling the rate of mass transfer (Ghibate *et al.* 2021).

3.5 Effect of temperature on metal retention and thermodynamics study

The adsorption equilibrium of Pb (II) on the (UC) and (PAC) adsorbents was studied in the range of 25 to 55°C, shown in Fig. 9. The result revealed that the adsorption capacity of Pb (II) ions onto the (UC) slightly decreases from $13.45 \text{ mg}\cdot\text{g}^{-1}$ to $13.28 \text{ mg}\cdot\text{g}^{-1}$ by increasing the temperature of the solution from 25°C to 55°C, thus indicating that the process of removing Pb (II) ions by (UC) is exothermic ($\Delta H < 0$).

The effect of the adsorption heat of Pb (II) ions on (UC) and (PAC) was determined using thermodynamic parameters, namely free energy change (ΔG°), The entropy change (ΔS°) and enthalpy charge (ΔH°) and were determined using Eqs. (10) and (11).

$$\ln K_d = ((\Delta S^\circ)/R) - ((\Delta H^\circ)/R) 1/T \quad (10)$$

$$\Delta G^\circ = -RT \ln K_d \quad (11)$$

where ($K_d = Q_e/C_e$) in ($\text{L}\cdot\text{g}^{-1}$) is the distribution constant or it is the ratio between the amount of adsorbate retained per 1g of solid and the concentration of adsorbate at equilibrium; R ($\text{J}\cdot\text{mol}^{-1}\cdot\text{K}^{-1}$) is the ideal gas constant and T(K) is the absolute temperature.

(ΔH°) and (ΔS°) were obtained from the slope and intercept of Van't Hoff's plot of $\ln K_d$ versus $1/T$ as shown in Fig. 9. (ΔG°) was calculated at different temperatures (25, 35, 45 and 55°C) using Eq. (11). The negative values of the three parameters ($\Delta H^\circ = -9.72 \text{ kJ}\cdot\text{mol}^{-1}$), ($\Delta G^\circ = -9.62, -9.74, -9.63 \text{ kJ}\cdot\text{mol}^{-1}$ for $T = 298, 308$ and 328 k respectively) and ($\Delta S^\circ = -0.17 \text{ j}\cdot\text{mol}^{-1}$) in the case of (UC) indicate that the adsorption process of Pb (II) ions is spontaneous, exothermic and that the order of distribution of the Pb (II) ions on the (UC) is important compared to that in the solution. Furthermore, an examination of the standard enthalpy value of adsorption ($\Delta H^\circ < 40 \text{ kJ}\cdot\text{mol}^{-1}$) shows that it is a physisorption mechanism. The negative (ΔS°) value shows that the adsorption occurs with increasing order at the solid-solution interface.

For (PAC), the calculation of standard adsorption free enthalpies (ΔG°) gave negative values in all cases indicating spontaneous adsorption. It was also noted that the use of the distribution coefficient (K_d) for the calculation of (ΔH°) and (ΔS°) is not appropriate, which gives a plot with a very low correlation coefficient ($r^2 = 0.18901$).

Similar observations have been reported by Tran and you (2016) in their study on the adsorption of cadmium ions on orange peel and by Alnajrani and Alsager (2020) in their work on the elimination of antibiotics from the water by an intrinsic microporosity polymer.

3.6 Adsorption isotherm models

The results obtained by plotting the curve giving the variation in the quantity of Pb (II) retained per gram of

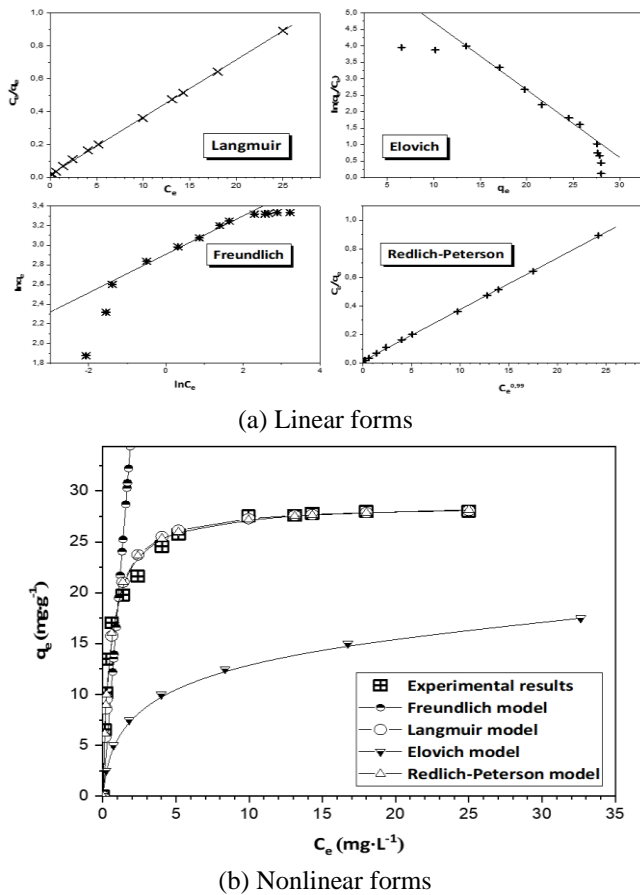


Fig. 11 Adsorption isotherms of Pb (II) ions on used cardboard

Table 3 Isotherm models applied for Pb (II) ions adsorption on (UC) and (PAC)

Isothermal models	Parameters	Parameter values	
		Used cardboard	Powdered activated carbon
Freundlich	n	5.1156	8.2980
	K_F [$\text{mg}\cdot\text{g}^{-1}(\text{L}\cdot\text{mg}^{-1})^{1/n}$]	18.3153	29.9811
	r^2	0.98825	0.99261
Langmuir	Q_m ($\text{mg}\cdot\text{g}^{-1}$)	28.64	41.70
	K_L ($\text{L}\cdot\text{mg}^{-1}$)	2.0208	2.2859
	r^2	0.99971	0.99953
Elovich	Q_m ($\text{mg}\cdot\text{g}^{-1}$)	4.86	3.70
	K_E ($\text{L}\cdot\text{mg}^{-1}$)	4.02427	22.97924
	r^2	0.99227	0.99475
Redlich – Peterson	Q_m ($\text{mg}\cdot\text{g}^{-1}$)	27.52	35.48
	n	0.99	0.97
	K_L ($\text{L}\cdot\text{mg}^{-1}$)	2.2965	5.37929
	r^2	0.99973	0.9997

adsorbent as a function of the concentration of Pb (II) ions in solution at equilibrium, allowed us to obtain the adsorption isotherm of Pb (II) on the two solids used.

To obtain the best fitting isotherm, the equilibrium data were analyzed using Langmuir, Freundlich, Elovich, and Redlich-Peterson.

Q_m , K_L , $1/n$, K_F , Q_e values were obtained by linear regression of the four models adopted to choose the one that can best express the results obtained experimentally and also describe the adsorption equilibrium characteristics of the Pb (II) ions on the (UC) and the (PAC). The validity of a theoretical model concerning the experimental results is based mainly on the regression coefficient r^2 closest to the unit and Q_e closest to that found experimentally.

The essential characteristics of the Langmuir equation can be expressed in terms of a dimensionless constant, called the equilibrium parameter R_L which is in direct relation with the initial concentration of Pb (II) ions and which indicates whether the adsorption is favorable or not according to this model. The R_L parameter is expressed by Eq. (12):

$$R_L = \frac{1}{1 + K_L C_0} \quad (12)$$

where K_L is the Langmuir constant (indicates the nature of the adsorption and the shape of the isotherm); C_0 represents the initial concentration in ($\text{mg}\cdot\text{L}^{-1}$).

The value of R_L indicates whether the type of isotherm observed is favorable ($0 < R_L < 1$), unfavorable ($R_L > 1$), linear ($R_L = 1$) or irreversible ($R_L = 0$) (Koswojo *et al.* 2010).

Fig. 10 represents the variation of R_L as a function of C_0 brought into contact with 0.14 g of (UC). It is noted that the calculated values of R_L , for all the initial concentrations involved for the study of the adsorption isotherm of Pb (II) on (UC) were located in the interval $0 < R_L < 1$, which corresponds to a favorable adsorption process.

The adsorption is considered favorable for the Freundlich model, when $0.1 < 1/n < 1$ (Karthikeyan *et al.* 2005), and the higher the values of $1/n$ better is the favorability of adsorption.

For the Redlich-Peterson isotherm model, Eq. (9) is reduced to the Freundlich isotherm with low surface coverage and the Langmuir isotherm with high adsorbate concentration (Milenkovic *et al.* 2013). The exponent n of Eq. (9) is between 0 and 1, for $n = 1$, the equation is reduced to the Langmuir isothermal model and for $n = 0$, it is reduced to the Henry equation (Kazak *et al.* 2015).

The four isotherms are modeled graphically in Fig. 11(a) and the parameters are mentioned in Table 3. Fig. 11(b) shows the comparison between the isothermal form found experimentally with the nonlinear forms of the equations corresponding to the applied models.

Examination of the results indicates that the Langmuir and Redlich-Peterson isotherms corresponded more precisely to the experimental results of the Pb (II) ions adsorption on (PAC) than the Freundlich and Elovich, isotherms, this is due not only to the high regression coefficient greater than 0.999 but also to the Q_m calculated very close to the quantity recorded experimentally ($41 \text{ mg}\cdot\text{g}^{-1}$).

According to the curves obtained from the nonlinear shapes (Fig. 11(b)), the isotherms data can be fitted well

with two models of nonlinear regression adsorption isotherms. The applicability of the Langmuir and Redlich-Peterson nonlinear equations can produce consistent results, even though the parameter values are not the same. The three-parameter equation (Redlich-Peterson) offers a better fit, similar to that obtained with the nonlinear two-parameter Langmuir equation, which is because the parameter n is very close to unity (0.97) which reduces the Redlich-Peterson equation to the Langmuir isothermal model. Consequently, the possible hypotheses linked to the phenomenon of Pb (II) ions retention by the (PAC) are those of the Langmuir model, which provides for monolayer adsorption on energetically homogeneous active sites and without interaction between the adsorbed cations of Pb.

For (UC), we notice from the results obtained by the linear forms of the applied isotherms that the Langmuir (monolayer adsorption) and Redlich-Peterson (multilayer adsorption) models have comparable correlation coefficients ($r^2 = 0.99971$ and $r^2 = 0.99973$, respectively). On the other hand, the adsorption capacities ($Q_{\max}^{\text{cal}} = 28.64 \text{ mg}\cdot\text{g}^{-1}$ and $27.52 \text{ mg}\cdot\text{g}^{-1}$) are almost identical to that determined experimentally ($Q_{\max}^{\text{exp}} = 28 \text{ mg}\cdot\text{g}^{-1}$).

For the curves obtained for nonlinear shapes, and especially for low concentrations, it is observed that more than one model can be valid to express the mode of retention.

The nonlinear forms of two models equations (Langmuir and Redlich-Peterson) pass through the majority of the experimental points, which suggests that the adsorption is, perhaps, not reflected by either of these models. All these results lead us to suppose that the retention mechanism in the (UC) which is characterized by a certain moderate surface area ($S = 1.0192 \text{ m}^2\cdot\text{g}^{-1}$) and low crystallinity, follows a certain distribution that remains to be elucidated.

4. Conclusions

The Pb (II) ions adsorption onto the used cardboard and powdered activated carbon were the main focus of this study. The results obtained showed that the two solids used are effective materials for the retention of Pb (II), with optimal doses of $1.4 \text{ g}\cdot\text{L}^{-1}$ and $0.8 \text{ g}\cdot\text{L}^{-1}$ for powdered activated carbon and used cardboard respectively for an initial concentration of $20 \text{ mg}\cdot\text{L}^{-1}$ in Pb (II) ions. The optimum pH for the retention of Pb (II) ions is around 5 for both adsorbents. The kinetics study indicates that the surface reaction is very fast with the used cardboard and the optimal time needed to reach equilibrium would be 10 minutes, and 20 minutes for powdered activated carbon. The thermodynamic parameters obtained indicate that the adsorption process is exothermic for the used cardboard with relatively weak interactions characteristic of a physisorption mechanism. For powdered activated carbon, the use of the distribution coefficient (K_d) gave a plot with a very low correlation coefficient which does not allow the calculation of (ΔH°) and (ΔS°). Of all the kinetic models tested on the experimental data, only the pseudo-second-order model describes all of our results. This study shows that Pb (II) sorption on the used cardboard and the powdered activated carbon is accompanied by intraparticle

diffusion and therefore by the contribution of active sites inside the pores, especially for powdered activated carbon. The adsorption isotherms seem to be well described by the Langmuir and Redlich-Peterson isotherms with n very close to 1 for both sorbents.

The adsorption of Pb (II) ions is significant on powdered activated carbon ($41 \text{ mg}\cdot\text{g}^{-1}$) compared to used cardboard ($28 \text{ mg}\cdot\text{g}^{-1}$). The adsorption efficiency of (PAC) highly depends on its textural properties. Indeed, it has a BET specific surface equal to $53.980 \text{ m}^2\cdot\text{g}^{-1}$ much higher than that of (UC) which is of the order of $1.0192 \text{ m}^2\cdot\text{g}^{-1}$, and total volume of pores whose diameter is less than 363.8 \AA equal at $0.05249 \text{ cm}^3\cdot\text{g}^{-1}$, very large compared to that recorded with the used cardboard which is $0.003640 \text{ cm}^3\cdot\text{g}^{-1}$.

The retention capacity/equilibrium time ratio is interesting for used cardboard ($2.8 \text{ mg}\cdot\text{g}^{-1}\cdot\text{min}^{-1}$) and then the powdered activated carbon ($2.02 \text{ mg}\cdot\text{g}^{-1}\cdot\text{min}^{-1}$).

Finally, despite the adsorption capacity of the used cardboard was not so impressive although its use has an advantage in terms of recirculation of resources, its availability in large quantities as the most abundant free waste in nature, can make this material an adsorbent suitable for large-scale use in the treatment of water polluted by heavy metals, after having studied the potential difficulties encountered with the manipulation of this material on the economic burden.

References

- Allen, S.J., McKay, G. and Khader, K.Y.H. (1989), "Intraparticle diffusion of a basic dye during adsorption onto sphagnum peat", *Environ. Pollut.*, **56**(1), 39-50.
[https://doi.org/10.1016/0269-7491\(89\)90120-6](https://doi.org/10.1016/0269-7491(89)90120-6).
- Alnajrani, M.N. and Alsager, O.A. (2020), "Removal of antibiotics from water by polymer of intrinsic microporosity: Isotherms, kinetics, thermodynamics, and adsorption mechanism", *Sci. Rep.*, **10**(1), 794.
<https://doi.org/10.1038/s41598-020-57616-4>.
- Alshameri, A., Yan, C. and Lei, X. (2014), "Enhancement of phosphate removal from water by TiO₂/Yemeni natural zeolite: Preparation, characterization and thermodynamic", *Micropor. Mesopor. Mater. J.*, **196**, 145-157.
<https://doi.org/10.1016/j.micromeso.2014.05.008>.
- Amarasinghe, B.M.W.P.K. and Williams, R.A. (2007), "Tea waste as a low-cost adsorbent for the removal of Cu and Pb from wastewater", *Chem. Eng. J.*, **132**(1-3), 299-309.
<https://doi.org/10.1016/j.cej.2007.01.016>.
- Ayyappan, R., Carmalin Sophia, A., Swaminathan, K. and Sandhya, S. (2005), "Removal of Pb (II) from aqueous solution using carbon derived from agricultural wastes", *Proc. Biochem.*, **40**(3-4), 1293-1299.
<https://doi.org/10.1016/j.procbio.2004.05.007>.
- Axtell, N.R., Sternberg, S.P. and Claussen, K. (2003), "Lead and nickel removal using microspora and lemna minor", *Bioresour. Technol.*, **89**(1), 41-48.
[https://doi.org/10.1016/S0960-8524\(03\)00034-8](https://doi.org/10.1016/S0960-8524(03)00034-8).
- Bai, S., Wang, T., Tian, Z., Cao, K. and Li, J. (2020), "Facile preparation of porous biomass charcoal from peanut shell as adsorbent", *Sci. Rep.*, **10**(1), 15845.
<https://doi.org/10.1038/s41598-020-72721-0>.
- Battas, A., El Gaidoumi, A., Ksakas, A. and Kherbeche, A. (2019), "Adsorption study for the removal of nitrate from water

- using local clay”, *Sci. World J.*, 2019, 9529618. <https://doi.org/10.1155/2019/9529618>.
- Bharathi, S.K. and Ramesh, P.S. (2012), “Equilibrium, thermodynamic and kinetic studies on adsorption of a basic dye by *Citrullus lanatus* rind”, *Iran J. Energ. Environ.*, **3**(1), 23-34. <https://doi.org/10.5829/idosi.ijee.2012.03.01.0130>.
- Bouberka, Z., Kacha, S., Kameche, M., Elmaleh, S. and Derriche, Z. (2005), “Sorption study of an acid dye from an aqueous solution using modified clays”, *J. Hazard. Mater.*, **119**(1-3), 117-124. <https://doi.org/10.1016/j.jhazmat.2004.11.026>.
- Boulaiche, W., Hamdi, B. and Trari, M. (2019), “Removal of heavy metals by chitin: Equilibrium, kinetic and thermodynamic studies”, *Appl. Water Sci.*, **9**(2), 39. <https://doi.org/10.1007/s13201-019-0926-8>
- Brião, G.D., de Andrade, J.R., da Silva, M.G.C. and Viera, M.C.A. (2020), “Removal of toxic metals from water using chitosan-based magnetic adsorbents”, *Environ. Chem. Lett.*, **18**(4), 1145-1168. <https://doi.org/10.1007/s10311-020-01003-y>.
- Chionyedua, T.O., Cosmas, C.U., Alechine, E.A. and Leslie, F.P. (2019), “Comparative study of the adsorption capacity of lead (II) ions onto bean husk and fish scale from aqueous solution”, *J. Water Reuse D.*, **9**(3), 249-262. <https://doi.org/10.2166/wrd.2019.061>.
- Crini, G. and Badot, P.M. (2010), *Sorption Processes and Pollution: Conventional and Non-Conventional Sorbents for Pollutant Removal From Wastewaters*, Presses Universitaires de Franche-Comté, Besançon, France.
- El-Ashtoukhy, E.S.Z., Amin, N.K. and Abdelwahab, O. (2008), “Removal of lead (II) and copper (II) from aqueous solution using Pomegranate Peel as a new adsorbent”, *Desalination*, **223**(1-3), 162-173. <https://doi.org/10.1016/j.desal.2007.01.206>.
- Elboughdiri, N. (2020), “The use of natural zeolite to remove heavy metals Cu (II), Pb (II) and Cd (II), from industrial wastewater”, *Cogent Eng.*, **7**(1), 1782623. <https://doi.org/10.1080/23311916.2020.1782623>.
- Elovich, S.Y. and Larionov, O.G. (1962), “Theory of adsorption from nonelectrolyte solutions on solid adsorbents”, *Russ. Chem. Bull.*, **11**(2), 198-203. <https://doi.org/10.1007/BF00908017>.
- Freundlich, H. (1907), “Über die adsorption in lösungen”, *Zeitschrift für Physikalische Chemie*, **57**(1), 385-470. <https://doi.org/10.1515/zpch-1907-5723>.
- Georgescu, A.M., Nardou, F., Zichil, V. and Nistor, I.D. (2018), “Adsorption of lead (II) ions from aqueous solutions onto Cr-pillared clays”, *Appl. Clay Sci.*, **152**, 44-52. <https://doi.org/10.1016/j.clay.2017.10.031>.
- Ghibate, R., Senhaji, O. and Taouil, R. (2021), “Kinetic and thermodynamic approaches on rhodamine b adsorption onto pomegranate peel”, *Case Stud. Chem. Environ. Eng.*, **3**, 1000782. <https://doi.org/10.1016/j.csee.2020.100078>.
- Hameed, B.H. (2009), “Evaluation of papaya seeds as a novel non-conventional low-cost adsorbent for removal of methylene blue”, *J. Hazard. Mater.*, **162**(2-3), 939-944. <https://doi.org/10.1016/j.jhazmat.2008.05.120>.
- Hana, J., Nohback, P. and Hyokwan, B. (2020) “Removal of Pb (II) from wastewater by biosorption using powdered waste sludge”, *Membr. Water Treat.*, **11**(1), 41-48. <https://doi.org/10.12989/mwt.2020.11.1.041>.
- Hashemian, S. (2011), “Kinetic and thermodynamic of adsorption of methylene blue (MB) by CuFe₂O₄/rice bran composite”, *Int. J. Phys. Sci.*, **6**(27), 6257-6267. <https://doi.org/10.5897/IJPS11.187>.
- Herawati, N., Suzuki, S., Hayashi, K., Rivai, I.F. and Koyoma, H. (2000), “Cadmium, copper, and zinc levels in rice and soil of Japan, Indonesia, and China by soil type”, *B. Environ. Contam. Tox.*, **64**(1), 33-39. <https://doi.org/10.1007/s001289910006>.
- Hospodarova, V., Singovszka, E. and Stevulova, N. (2018), “Characterization of cellulosic fibers by FTIR spectroscopy for their further implementation to building materials”, *Am. J. Anal. Chem.*, **9**(6), 303-310. <https://doi.org/10.4236/ajac.2018.96023>.
- Ho, Y.S. and McKay, G. (1999), “Pseudo-second order model for sorption processes”, *Proc. Biochem.*, **34**(5), 451-465. [https://doi.org/10.1016/S0032-9592\(98\)00112-5](https://doi.org/10.1016/S0032-9592(98)00112-5).
- Jeongmin, H., Seungwoo, L., Dongah, K., Eunmi, K. and Yuhoon, H. (2020), “Improved adsorption performance of heavy metals by surface modification of polypropylene/polyethylene media through oxygen plasma and acrylic acid”, *Membr. Water Treat.*, **11**(3), 231-235. <https://doi.org/10.12989/mwt.2020.11.3.231>.
- Kanan, K. and Sundaram, M.M. (2001), “Kinetics and mechanism of removal methylene blue by adsorption on the various carbons-a comparative study”, *Dyes Pigments*, **51**(1), 25-40. [https://doi.org/10.1016/S0143-7208\(01\)00056-0](https://doi.org/10.1016/S0143-7208(01)00056-0)
- Karthikeyan, T., Rajgopal, S., and Miranda, L.R. (2005), “Chromium (VI) adsorption from aqueous solution by hevea brasiliensis sawdust activated carbon”, *J. Hazard Mater.*, **124**(1-3), 92-199. <https://doi.org/10.1016/j.jhazmat.2005.05.003>.
- Kataria, N., Garg, V.K., Jain, M. and Kadirvelu, K. (2016), “Preparation, characterization and potential use of flower shaped Zinc oxide nanoparticles (ZON) for the adsorption of Victoria Blue B dye from aqueous solution”, *Adv. Powder Technol.*, **27**(4), 1180-1188. <https://doi.org/10.1016/j.apt.2016.04.001>.
- Kazak, O., Tor, A., Akin, I. and Arslan, G. (2015), “Preparation of new polysulfone capsules containing Cyanex 272 and their properties for Co (II) removal from aqueous solution”, *J. Environ. Chem. Eng.*, **3**(3), 1654-1661. <https://doi.org/10.1016/j.jece.2015.06.007>.
- Koswojo, R., Utomo, R.P., Ju, Y.H., Ayucitra, A., Soetaredjo, F.E., Sunarso, J. and Ismadji, S. (2010), “Acid green 25 removal from wastewater by organo-bentonite from pacitan”, *Appl. Clay Sci.*, **48**(1-2), 81-86. <https://doi.org/10.1016/j.clay.2009.11.023>.
- Lagergren, S (1898), “Zur theorie der sogenannten adsorption geloster stoffe”, *Kungliga Svenska Vetenskapsakademiens Handlingar*, **24**(1), 1-39.
- Langmuir, I. (1918), “The adsorption of gases on plane surfaces of glass, mica, and platinum”, *J. Am. Chem. Soc.*, **40**(9), 1361-1403. <https://doi.org/10.1021/ja02242a004>.
- Maier, R.S. and Schure, M.R. (2018), “Transport properties and size exclusion effects in wide-pore superficially porous particles”, *Chem. Eng. Sci.*, **185**, 243-255. <https://doi.org/10.1016/j.ces.2018.03.041>.
- McKay, G., Otterburn, M.S. and Sweeney, A.G. (1980), “The removal of colour from effluent using various adsorbents—IV. Silica: Equilibria and column studies”, *Water Res.*, **14**(1), 21-27. [https://doi.org/10.1016/0043-1354\(80\)90038-X](https://doi.org/10.1016/0043-1354(80)90038-X).
- Mekhalef Benhafsa, F., Kacha, S., Leboukh, A. and et Belaid, K.D (2018) “Étude comparative de l’adsorption du colorant Victoria Bleu Basique à partir de solutions aqueuses sur du carton usagé et de la sciure de bois”, *J. Water Sci.*, **31**(2), 109-126. <https://doi.org/10.7202/1051695ar>.
- Milenkovic, D.D., Milosavljevic, M.M., Marinkovic, A.D., Đokic, V.R., Mitrovic, J.Z. and Ljbojic, A.R (2013), “Removal of copper (II) ion from aqueous solution by high-porosity activated carbon”, *Water S.A.*, **39**(4), 515-522. <https://doi.org/10.4314/wsa.v39i4.10>.
- Mohammadi, S.Z., Karimi, M.A., Afzali, D. and Mansouri, F. (2010), “Removal of Pb (II) from aqueous solutions using activated carbon from sea-buckthorn stones by chemical activation”, *Desalination*, **262**(1-3), 86-93. <https://doi.org/10.1016/j.desal.2010.05.048>.
- Nejadshafie, V. and Islami, M.R. (2019), “Adsorption capacity of heavy metal ions using sultone-modified magnetic activated carbon as a bio-adsorbent”, *Mater. Sci. Eng. C*, **101**, 42-52.

- <https://doi.org/10.1016/j.msec.2019.03.081>.
- Obayomi, K.S., Bello, J.O., Nnoruka, J.S., Adediran, A.A and Olajide, P.O. (2019), "Development of low-cost bio-adsorbent from agricultural waste composite for Pb (II) and As (III) sorption from aqueous solution", *Cogent Eng.*, **6**(1), 1687274. <https://doi.org/10.1080/23311916.2019.1687274>.
- Özcan, A., Öncü, E.M. and Özcan, A.S. (2006), "Kinetics, isotherm and thermodynamic studies of adsorption of Acid Blue 193 from aqueous solutions onto natural sepiolite", *Colloid Surfaces A.*, **277**(1-3), 90-97. <https://doi.org/10.1016/j.colsurfa.2005.11.017>.
- Ponnusamy, S.K. and Subramaniam, R. (2013), "Process optimization studies of Congo red dye adsorption onto cashew nutshell using response surface methodology", *Int. J. Ind. Chem.*, **4**(1), 17. <https://doi.org/10.1186/2228-5547-4-17>.
- Rashed, M.N., Gad, A.A. and Abdeldaiem, A.M. (2018), "Preparation and characterization of green adsorbent from waste glass and its application for the removal of heavy metals from well water", *Adv. Environ. Res.*, **7**(1), 53-71. <https://doi.org/10.12989/aer.2018.7.1.053>
- Redlich, O. and Peterson, D.L. (1959), "A useful adsorption isotherm", *J. Phys. Chem.*, **63**(6), 1024. <https://doi.org/10.1021/j150576a611>.
- Sepulveda, L.A. and Santana, C.C. (2013), "Effect of solution temperature, pH and ionic strength on dye adsorption onto Magellanic peat", *J. Environ. Tech.*, **34**(8), 967-977. <https://doi.org/10.1080/09593330.2012.724251>.
- Shaban, M., Abukhadra, M.R., Parwaz, A.A. and Jabili, B.M. (2018), "Removal of Congo red, methylene blue and Cr (VI) ions from water using natural serpentinite", *J. Taiwan Inst. Chem. Eng.*, **82**, 102-116. <https://doi.org/10.1016/j.jtice.2017.10.023>.
- Shirsath, D.S. and Shrivastava, V.S. (2012), "Removal of hazardous dye Ponceau-S by using chitin: An organic bioadsorbent", *Afr. J. Environ. Sci. Technol.*, **6**(2), 115-124. <https://doi.org/10.5897/AJEST11.118>.
- Simonin, J.P. (2016), "On the comparison of pseudo-first-order and pseudo-second-order rate laws in the modeling of adsorption kinetics", *Chem. Eng. J.*, **300**, 254-263. <https://doi.org/10.1016/j.cej.2016.04.079>.
- Sparks, D.L. (2003), *Environmental Soil Chemistry*, Elsevier, California, U.S.A.
- Sreejalekshmi, K.G., Krishnan, K.A. and Anirudhan, T.S. (2009), "Adsorption of Pb (II) and Pb (II)-citric acid on sawdust activated carbon: Kinetic and equilibrium isotherm studies", *J. Hazard. Mater.*, **161**(2-3), 1506-1513. <https://doi.org/10.1016/j.jhazmat.2008.05.002>.
- Srivastava, V.C., Swamy, M.M., Mall, I.D., Prasad, B. and Mishra, I.M. (2006), "Adsorptive removal of phenol by bagasse fly ash and activated carbon: Equilibrium, kinetics, and thermodynamics", *Colloid Surface A.*, **272**(1-2), 89-104. <https://doi.org/10.1016/j.colsurfa.2005.07.016>.
- Tran, H.N., You, S.J. and Chao, H.P. (2016), "Thermodynamic parameters of cadmium adsorption onto orange peel calculated from various methods: A comparison study", *J. Environ. Chem. Eng.*, **4**(3), 2671-2682. <https://doi.org/10.1016/j.jece.2016.05.009>.
- Weber, Jr. W.J. and Morris, J.C. (1963), "Kinetics of adsorption on carbon from solution", *J. Sanit. Eng. Div.*, **89**(2), 31-59. <https://doi.org/10.1061/JSEDAI.0000430>
- Xia L., Huang, Z., Zhong, L., Xie, F., Tang, C. and Tsui, C. (2018), "Bagasse cellulose grafted with an amino-terminated hyperbranched polymer for the removal of Cr (VI) from aqueous solution", *J. Polym.*, **10**(8), 931. <https://doi.org/10.3390/polym10080931>.